

# An experimental study of the effect of wall temperature nonuniformity on natural convection in an enclosure heated from the side

P. Filis and D. Poulikakos\*

An experimental study of natural convection in a parallelepipedal enclosure induced by a single vertical wall is described. The upper half of this wall was warm and the lower half cold. The other enclosure walls were insulated. The temperature and flow measurements were performed in the high Rayleigh number regime ( $10^{10} < Ra < 5 \times 10^{10}$ ) by using water as the working fluid. The Rayleigh number was based on the enclosure height and the temperature difference between the warm and the cold part of the driving wall. The flow field featured two flat cells, one filled with warm fluid along the top horizontal wall, and the other filled with cold fluid along the bottom horizontal wall. Each of these cells was surrounded by an additional cell as tall as half the enclosure height. The above flow structure prohibited extensive thermal contact between warm and cold fluid, thus limiting the role of convection on the heat transfer process in the cavity. The findings of this study differ significantly from the findings of previous studies based on the 'classical' enclosure model possessing two isothermal vertical walls, the one warm and the other cold, and support the view that the use of 'more realistic' temperature boundary conditions in enclosure natural convection needs careful examination.

**Keywords:** *natural convection, wall temperature nonuniformity, parallelepipedal enclosure*

## Introduction

Fundamental research in enclosure natural convection with applications to energy conservation in buildings, cooling of electronic equipment, solar engineering, and environmental and geothermal fluid dynamics has triggered the interest of many investigators over the last few decades. Two important classes of problems, with respect to the thermal boundary conditions in the enclosure walls, can be clearly identified: (a) heating from below, and (b) heating from the side. Since the present study deals with heating from the side, the main focus of the introductory section is on this class of problems.

The majority of existing studies on natural convection in enclosures heated from the side focuses on the rectangular enclosure, by investigating a simple model which features isothermal or uniform flux vertical walls (one warm and the other cold) and adiabatic horizontal walls. A plethora of studies has been published based on the above model. The reported studies are both theoretical and experimental in nature, and they document the main heat and fluid flow characteristics in

the cavity both qualitatively and quantitatively. Comprehensive summaries of the existing work on the above problem are available in a number of review papers<sup>1-3</sup> and a recent heat transfer textbook<sup>4</sup>.

In many engineering applications, often the situation arises where non-uniform thermal boundary conditions are imposed on a single wall. For example, building walls are rarely isothermal, and, more often than not, they possess warm and cold regions. Similar situations can be found in packaged electronic equipment and heat exchangers. These non-uniform conditions along a single wall may seriously affect the heat and fluid flow phenomena in the enclosure. To exemplify, a recent investigation of natural convection in an inclined rectangular box with the top surface cold and the bottom surface half-heated and half-insulated<sup>5</sup> showed that the nonisothermality of the bottom wall affected significantly the size and strength of the flow cells in the box and yield temperature and flow fields noticeably different from those of the 'inclined Benard' problem.

The present paper reports what, we believe, constitutes the first experimental study on the effect of the existence of warm and cold regions along a vertical wall of an enclosure. To isolate this effect, the other enclosure walls are made adiabatic. It is shown that the natural convection phenomenon evolving in the enclosure differs

\* Department of Mechanical Engineering, University of Illinois at Chicago, PO Box 4348, Chicago, IL 60680, USA

Received 11 October 1985 and accepted for publication on 21 March 1986

fundamentally from the well-known results for the model which assumes that the two opposite vertical walls of the cavity are differentially heated<sup>1-4</sup>.

The experimental investigation outlined in the following sections focuses on the situation where the upper half of the driving wall is warm while the lower half is cold. This situation yields a stable thermal stratification in the cavity. The buoyancy-induced flow field features two vivid flat cells: one along the top wall filled with warm fluid, and the other along the bottom wall filled with cold fluid. These two cells communicate thermally predominately by conduction in the vertical direction (Fig 1). A jet of fluid travelling horizontally toward the differentially heat wall was also observed at the midheight of the enclosure. This jet replaces the fluid directed upward and downward through the boundary layers along the warm and the cold portions of the driving wall, respectively. The flow was laminar even in the highest Rayleigh number examined in the present study ( $Ra = 4.45 \times 10^{10}$ ). All the temperature and flow visualization measurements were conducted in the high Rayleigh number regime ( $10^{10} < Ra < 5 \times 10^{10}$ ) by using water as the working fluid.

### Experimental apparatus

The experimental apparatus was a parallelepipedal box, drawn to scale in Fig 2. The main dimensions of the box were  $L = 610$  mm,  $H = W = 457$  mm. The height-to-length aspect ratio of the enclosure was, therefore,  $H/L = 0.749$ . All five adiabatic walls of the enclosure were

constructed out of a plexiglass sheet of thickness 19 mm. The differentially heated vertical wall was constructed out of aluminium. In order to create a warm region on this wall, two electrical strip heaters capable of dissipating a maximum power of 800 W were installed on the upper half of the plate. Before clamping to the plate, a thin layer of highly conductive silicone paste was applied to the bottom of each heater. The heat generated electrically in the upper part of the wall was removed by circulating precooled alcohol in the cooling jacket which constitutes the lower part of the wall. The temperature of

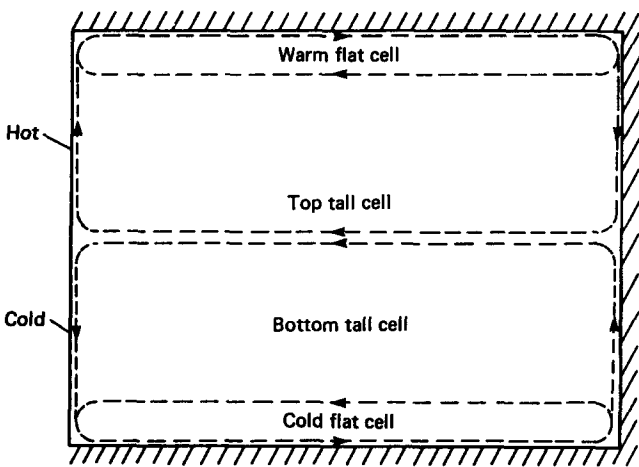


Fig 1 Schematic illustration of the flow pattern in the enclosure

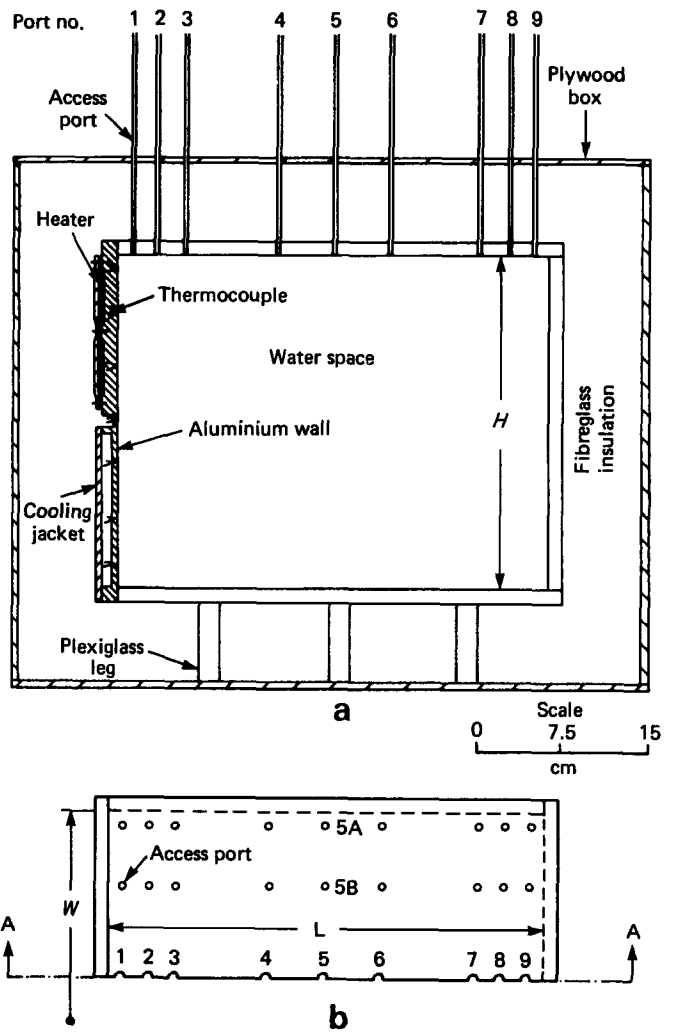


Fig 2 The experimental apparatus drawn to scale: (a) front view of section A-A; (b) top view

### Notation

$c_p$	Specific heat, J/kg K
$g$	Gravitational acceleration, m/s <sup>2</sup>
$H$	Height of the enclosure, m
$k$	Thermal conductivity, W/m K
$L$	Length of the enclosure, m
$Nu$	Nusselt number, Eq (1)
$Q$	Net heat transfer rate to the fluid, W, Eq (1)
$Ra$	Rayleigh number $\equiv g\beta\Delta TH^3/\nu\alpha$
$T$	Temperature, K
$\Delta T$	Temperature difference $\equiv T_H - T_C$
$\Delta t$	Time interval, s

$W$	Width of the enclosure, m
$\alpha$	Thermal diffusivity $\equiv k/(\rho c_p)$ , m <sup>2</sup> /s
$\beta$	Coefficient of thermal expansion, K <sup>-1</sup>
$\nu$	Kinematic viscosity, m <sup>2</sup> /s
$\rho$	Density, kg/m <sup>3</sup>

### Subscripts

C	Cold
H	Hot

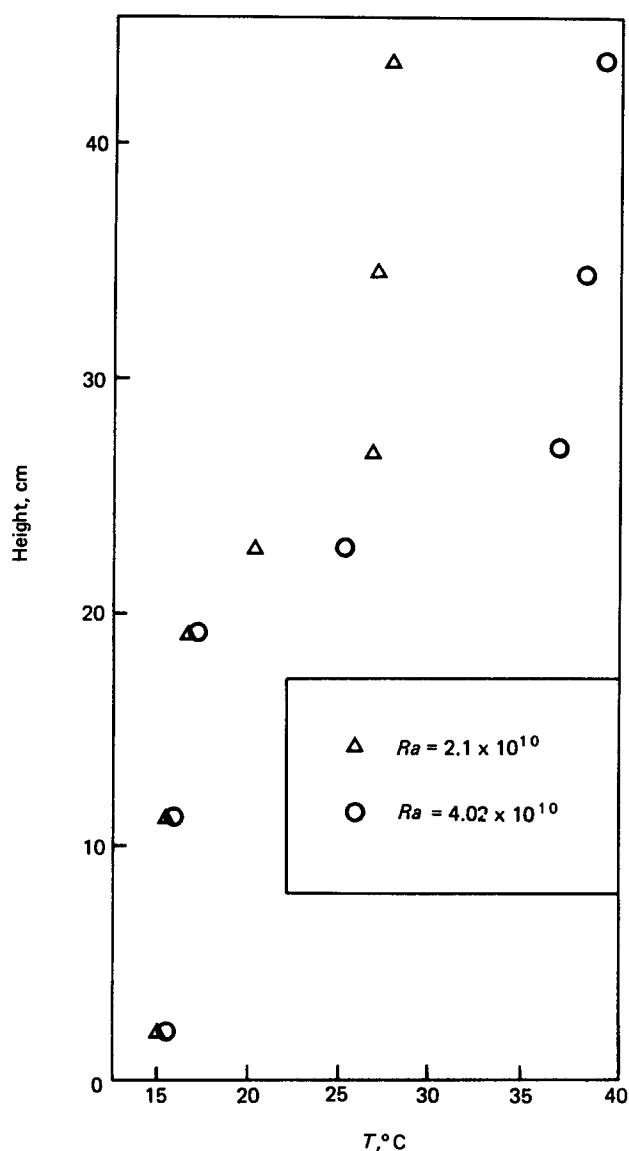


Fig 3 Temperature distribution in the vertical on the driving wall

the alcohol at the inlet of the cooling jacket was controlled within  $0.1^\circ\text{C}$  with the help of a bath refrigerator. To ensure isothermal conditions on the lower part of the wall the flow in the cooling jacket was distributed by using small baffles and following a trial and error procedure. This procedure was tedious, but eventually the cold part of the wall was made acceptably isothermal (within  $1^\circ\text{C}$ ). The warm part of the wall was also isothermal within  $1^\circ\text{C}$ . The temperature distribution on the aluminium plate in the vertical is illustrated in Fig 3 for two typical cases. Clearly, the temperature distribution of the wall changes from hot to cold over a short distance compared with the height of the cavity and constitutes a reasonably good approximation to a 'step' change in the wall temperature. The creation of this temperature distribution was aided by the fact that thermal communication between the warm and the cold parts of the wall was minimized by reducing (machining down) the plate thickness at midheight to as little as was safe to avoid cracking (3 mm). The temperature on the driving wall was monitored with thermocouples. Twenty-one chromel-alumel thermocouples were embedded in

the aluminium plate at a distance 1 mm from the surface facing the inside of the enclosure. Seven thermocouples were placed along the vertical centreline of the plate, seven at a distance 200 mm to the right of the centreline, and seven at a distance 200 mm to the left of the centreline. The exact spacing of the thermocouples in the vertical can be deduced from Fig 3. The thermocouple junction heads in the aluminium plate were plotted in silver epoxy to assure good thermal contact.

The experiments were performed using distilled water as the working fluid. A sequence of steady states was achieved by varying the electric heat input to the warm portion of the wall and keeping the temperature of cold portion constant. Power to the heaters was supplied by a DC power supply. As shown in Figs 2(a) and 2(b), forty-five access ports were drilled on the top wall of the apparatus for the temperature and velocity measurements. The access ports were connected to thin (3 mm inside diameter) vertical plexiglass tubes. The apparatus was insulated on all sides with 200 mm of fibreglass insulation surrounded by an outer plywood container of 15 mm wall thickness. On three of the side walls of the plywood container, windows were constructed. During the flow visualization measurements these windows were opened and the insulation sheet covering the plexiglass side walls was removed in order to allow photographing of the flow in the cavity. This operation had no effect on the study for it lasted only 1 or 2 minutes, which is extremely fast compared with the time scales in enclosure natural convection (our experiment required approximately 24 h to reach steady state).

### Temperature measurements

The temperature field inside the enclosure was determined with the help of a variable-depth chromel-alumel thermocouple probe of 0.5 mm bead diameter. To construct the probe a thermocouple was sealed inside a stiff capillary stainless steel tube. The thermocouple bead was located at the one end of the capillary tube and was able to come in direct contact with the fluid in the cavity and thus measure its temperature. The probe was lowered to any desired depth inside the enclosure through the access ports on the top wall.

Representative steady state temperature results are shown in Figs 4–6 for  $Ra = 2.1 \times 10^{10}$ ,  $Ra = 2.1 \times 10^{10}$ , and  $Ra = 4.02 \times 10^{10}$ , respectively. The flow field at these high Rayleigh numbers was laminar. Fig 4 illustrates a case of practically symmetric heating and cooling about the midheight of the driving wall. The temperature field in the cavity consists of three distinct regions:

- an isothermal 'cold' region occupying the vicinity of the bottom wall;
- an isothermal 'warm' region occupying the vicinity of the top wall;
- an almost linearly stratified region bridging the gap between regions (a) and (b).

It is worth noting that the temperature profiles exhibit minimal dependence on the distance from the driving wall. In addition, the temperature field was remarkably two-dimensional. To verify this fact it should be noted that the temperature profile under port 5B (denoted with triangles in Fig 4) hardly differs from the temperature profile under port 5. Additional temperature

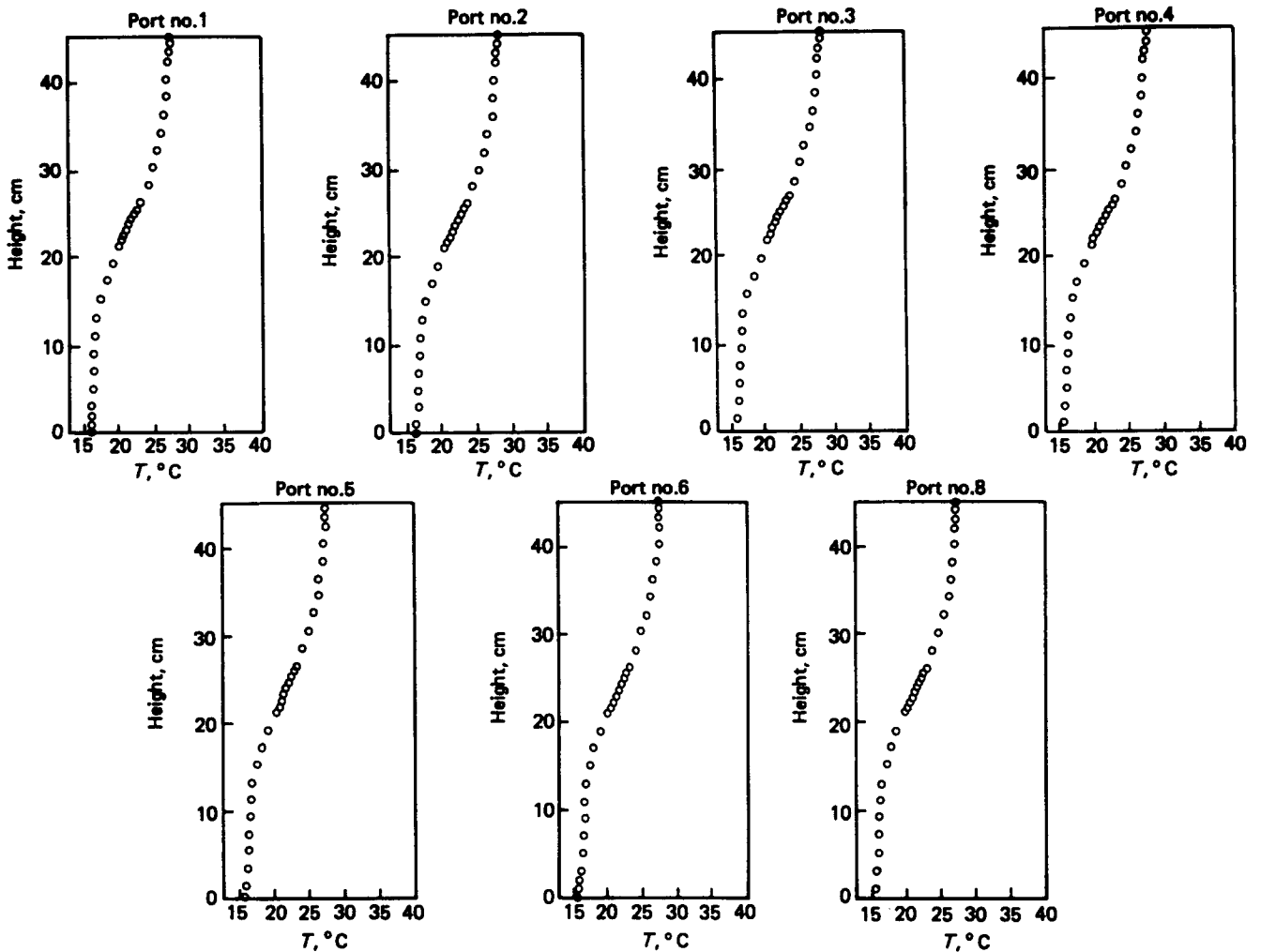


Fig 4 Vertical temperature profiles,  $Ra = 2.1 \times 10^{10}$

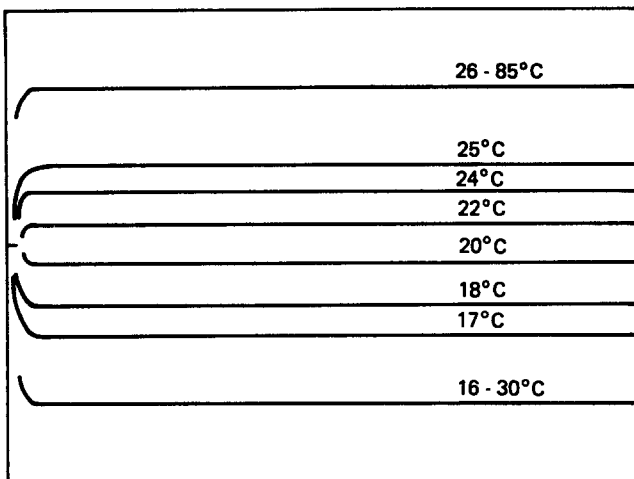


Fig 5 Pattern of isotherms,  $Ra = 2.1 \times 10^{10}$

measurements closer to the side walls (port 5A) as well as closer to the driving wall (ports 2A, 2B) did not noticeably alter the picture shown in Fig 4. A map of isotherms based on the temperature profiles of Fig 4 is shown in Fig 5. The basic feature of the temperature field revealed in this figure is that two sharp thermal boundary layers originating at midheight occupy the vicinity of the aluminium wall. Outside these thermal boundary layers

the temperature distribution is practically independent of horizontal position.

The temperature measurements presented in Fig 6 were obtained by increasing the power input to the heaters (compared with the power input used in Fig 4) while keeping the temperature of the lower half of the wall practically unchanged. As a result, the fluid occupying the upper part of the cavity reaches steady state at a higher temperature. In addition, a substantial increase in the slope of the temperature profile in the region away from the two horizontal walls is observed. This fact makes sense physically, for now a larger heat transfer rate is conducted through this region. Apart from the above, no other significant difference was observed between the temperature fields reported in Figs 4 and 6.

### Flow visualization and velocity measurements

The flow was visualized by using the thymol blue pH-indicator technique introduced by Baker<sup>6</sup> and successfully used in numerous natural convection experiments<sup>7-10</sup>. In this experiment two vertical stainless steel electrodes (0.8 mm diameter) were lowered in the enclosure through two neighbouring access ports. Next, a small dc voltage (approximately 12 V) from a dry-cell source was applied between the electrodes. The hydrogen thus generated at the cathode causes a local increase in

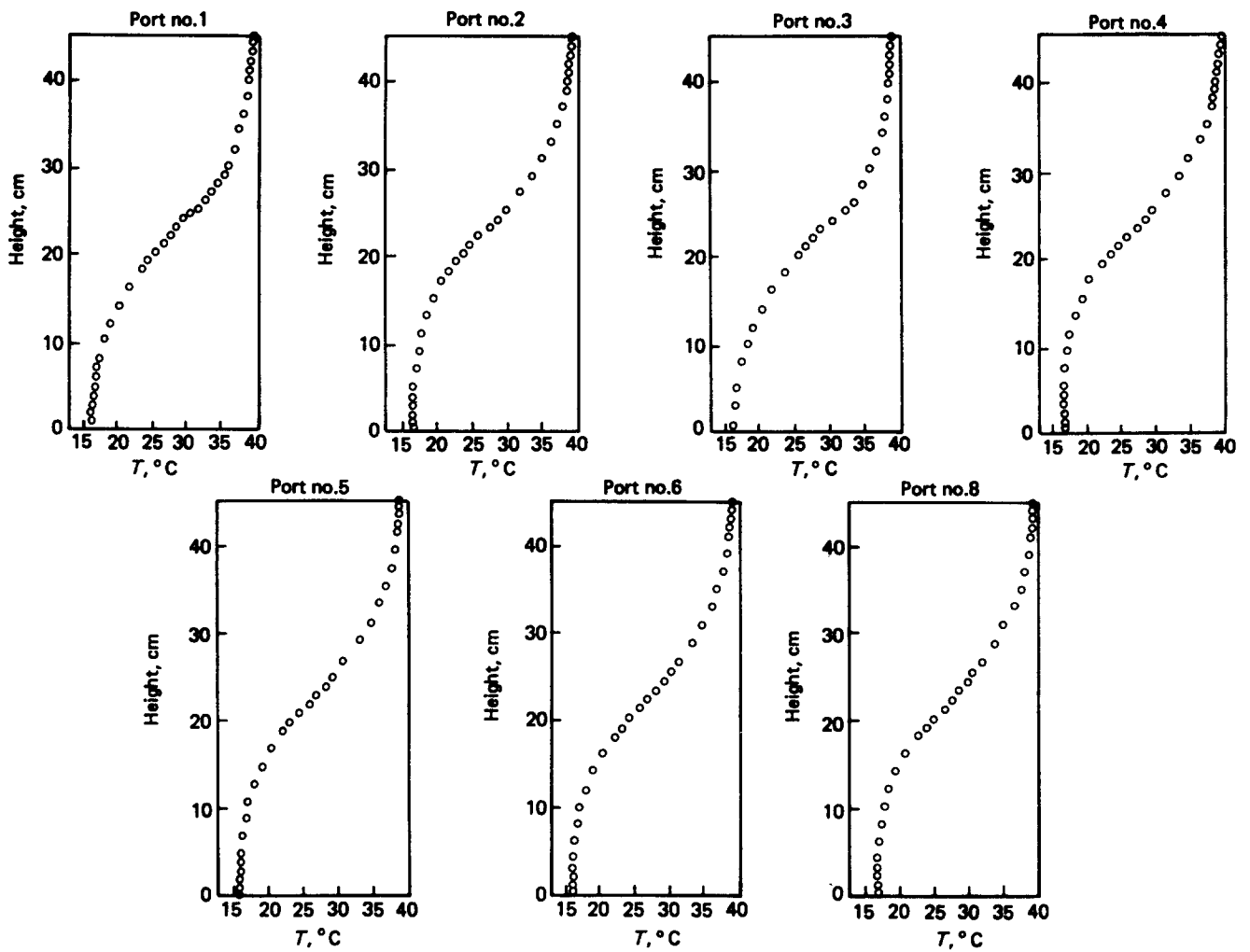


Fig 6 Vertical temperature profiles,  $Ra = 4.02 \times 10^{10}$

the pH of the fluid (water-thymol-blue solution) and changes its colour from yellow-orange to dark blue. The dark streak is neutrally buoyant and follows the motion of the fluid. As shown by the sequence of photographs in Fig 7, the evolution of the dark fluid in time is used to calculate the velocity field. The procedure for calculating the velocity field as well as a reliable calibration curve for the velocity probe are reported in detail elsewhere<sup>7,11</sup>. The flow visualization procedure described above made it clear that the flow field in the enclosure was indeed two-dimensional. The photographs in Fig 7 help to illustrate this fact.

Velocity profiles in the vertical for two different values of the Rayleigh number ( $Ra = 2.1 \times 10^{10}$  and  $4.02 \times 10^{10}$ ) are shown in Figs 8 and 9. Note that the values of  $Ra$  in Figs 8 and 9 are identical to the values of  $Ra$  in Figs 4 and 6, respectively, in which temperature measurements were reported. Fig 8 shows that the circulation in the enclosure features two 'flat' cells, one occupied by warm fluid and the other occupied by cold fluid, moving along the top and the bottom walls of the enclosure, respectively. The top cell consists of two warm jets travelling in opposite directions. The upper jet is a continuation of the warm stream flowing upwards along the driving wall. The lower jet is induced by the upper jet in a manner similar to a horizontal jet issuing into a thermally stratified pool<sup>12,13</sup>. The velocity profiles also

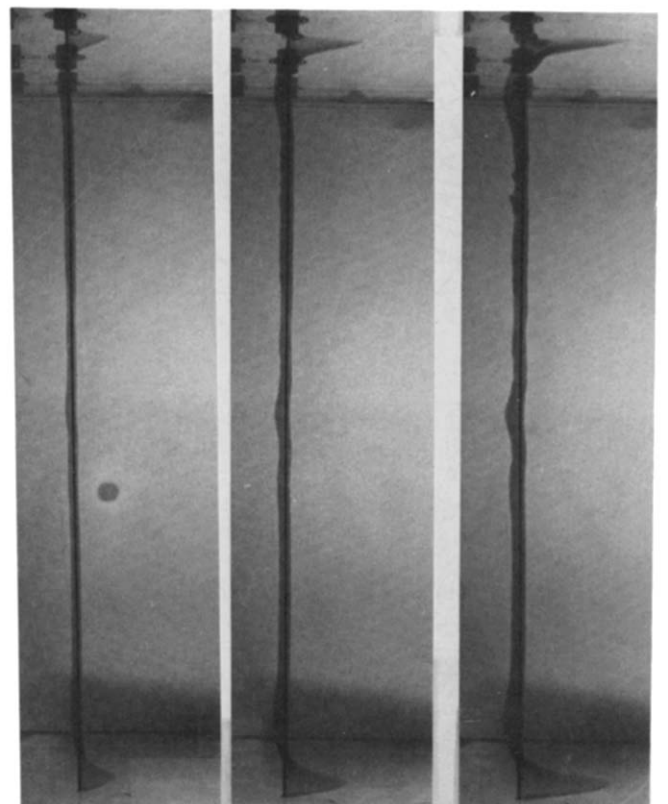


Fig 7 Flow visualization under port 3. The picture to the left was taken at  $t = 60$  s. The remaining two pictures were taken at time intervals  $\Delta t = 60$  s

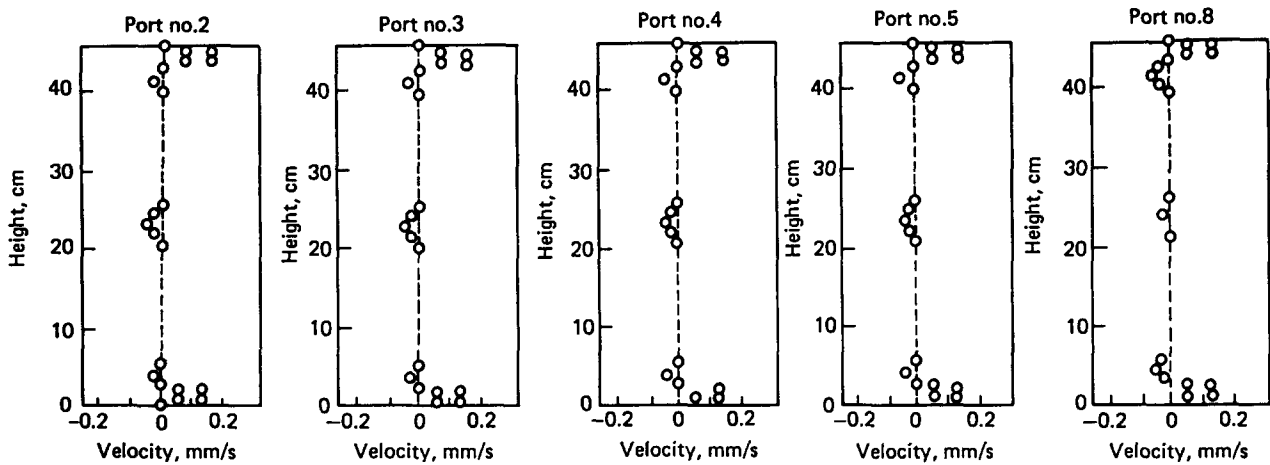


Fig 8 Velocity distribution in the vertical,  $Ra = 2.1 \times 10^{10}$

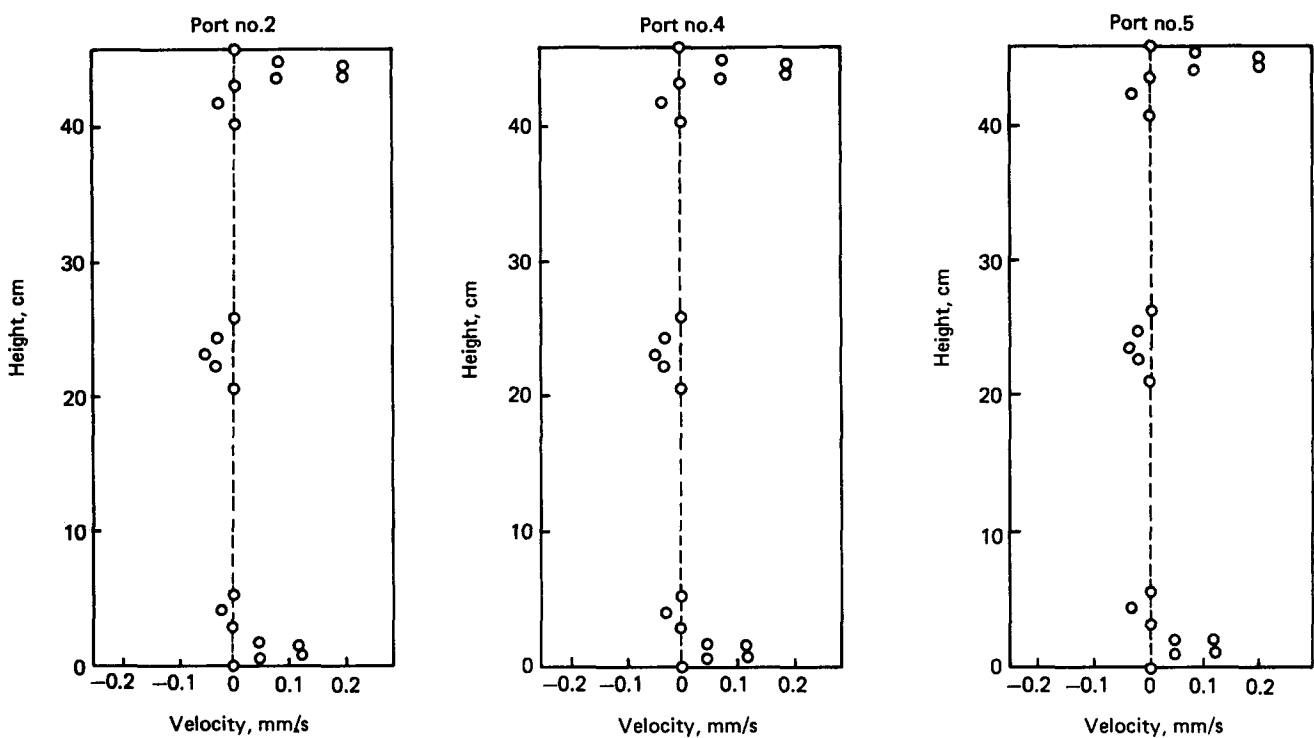


Fig 9 Velocity distribution in the vertical,  $Ra = 4.02 \times 10^{10}$

show a decrease in the velocity of the top jet away from the left wall, accompanied by an increase in the velocity of the lower jet. Similar arguments hold for the bottom wall cell. The rest of the fluid is practically stagnant, except for a thin region of slowly moving fluid located at the midheight of the cavity. This fluid travels toward the driving aluminium wall to replace the cold fluid falling along the cold portion, and the warm fluid rising along the warm portion, of this wall. It is worth noting that slow fluid motion along the right (adiabatic) vertical wall of the enclosure was also observed; however, it was difficult to photograph. In particular, two slowly moving streams, one falling from the top and the other rising from below, meet around the midheight, and after that they travel horizontally to the left, thus creating the jet discussed above. Fig 9 exhibits the same qualitative behaviour as Fig 8, only in this case the fluid velocity along the top wall is higher than the fluid velocity along the bottom wall.

In conclusion, the flow visualization experiments in the enclosure revealed a flow field drastically different from the well-known, basically unicellular flow field of the classical model<sup>1-4</sup>. The configuration under examination exhibits four cells, two strong and flat along the horizontal walls and two weak and as tall as half the enclosure height. The tall cells surround the flat cells. Since much of the cold fluid is trapped along the bottom of the cavity and much of the warm fluid is trapped along the top of the cavity, direct thermal contact between hot and cold fluid is, to a large extent, avoided.

### Heat transfer results

The net heat transfer rate through the enclosure was calculated for a series of steady states and is reported in Fig 10 by means of a Nusselt number versus Rayleigh number plot, where

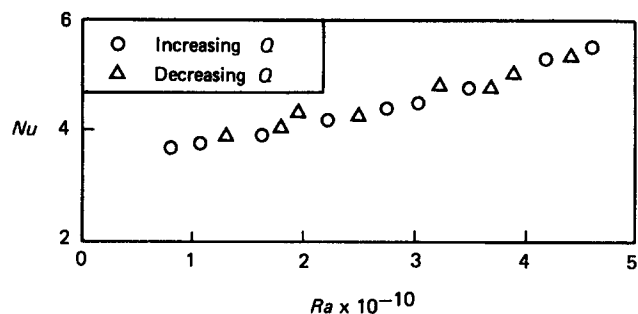


Fig 10 Heat transfer results

$$Nu = \frac{Q}{Wk\Delta T} \quad (1)$$

For each steady state in the apparatus, we measured the temperature of the warm and cold region of the driving wall using nine of the thermocouples located in each region (Fig 3). The arithmetic means of the measured local temperatures were used as the warm region and cold region temperatures. The physical properties appearing in the definition of  $Nu$  and  $Ra$  were evaluated at the arithmetic mean temperature of the warm and cold halves of the aluminium wall. The net heat transfer to the fluid was measured by first recording the electrical power to the strip heaters (voltage across the heaters multiplied by current through the heaters), and, next, by correcting this measurement to account for the heat leak by conduction to the cold region of the plate. The heat leak to the cold part of the aluminium plate was estimated by using Fourier's law and the information for the temperature distribution on the wall exemplified by Fig 4. Thus, the measured heat transfer rate to the fluid includes radiation effects which are negligible in the temperature range of the experiment.

To calculate the heat leak through the insulation blanket surrounding the apparatus a separate experiment was performed. During this experiment there was no coolant in the jacket of the cold portion of the aluminium, so that the electric heat input in the cavity was balanced by leakage of heat across the fibreglass insulation surrounding the apparatus. It was found that the heat leakage through the insulation was negligible (approximately 3 percent).

The main heat transfer results are reported graphically in Fig 10, where the relatively weak dependence of  $Nu$  on  $Ra$  is indicated. In addition, the data shown in Fig 10 are correlated by

$$Nu = 8.14 \times 10^{-3} Ra^{0.265} ; 10^{10} < Ra < 5 \times 10^{10} \quad (2)$$

As a final check, we reproduced our heat transfer data by running the experiment in the reverse direction, ie by gradually decreasing the power dissipated in the heaters by keeping the coolant temperature constant. Fig 10 shows that the  $Nu$  versus  $Ra$  measurements do not depend on the direction of the experiment.

### Conclusions

An experimental study of natural convection in a parallelepipedal enclosure driven by a single vertical wall with a cold and a warm region is reported. The cold region was positioned below the warm region. The study

focused on the high Rayleigh number regime  $10^{10} < Ra < 5 \times 10^{10}$ . The following conclusions were drawn.

- (1) The velocity field in the cavity (shown diagrammatically in Fig 1) consists of four cells, in contrast with the basically unicellular flow field in rectangular enclosures differentially heated in the horizontal direction.
- (2) The temperature field features two sharp thermal boundary layers covering the driving wall (Fig 5). In addition, the vicinity of the top wall is occupied by warm fluid while the vicinity of the bottom wall is occupied by cold fluid. The intermediate region is almost linearly stratified.
- (3) The flow structure in the enclosure inhibits direct thermal contact between warm and cold fluid. Thus, the dependence of the Nusselt number on  $Ra$  is relatively weak (Eq (2) and Fig 10).
- (4) Non-uniformities in the wall temperature, such as the one examined in this paper, may drastically affect the heat and fluid flow characteristics in enclosure natural convection in a desired or undesired manner, depending on the application. Hence, such non-uniformities deserve the researcher's scrutiny.

Finally, it is worth noting that in a recent theoretical and numerical investigation of the same problem<sup>14</sup> limited to the low Rayleigh number regime ( $Ra < 10^5$ ) it was shown that the temperature field in the enclosure transforms from one of incomplete vertical thermal penetration to one of incomplete horizontal thermal penetration, depending on the values of  $Ra$  and  $H/L$ . For example, for fixed  $Ra$ , tall enclosures may exhibit incomplete vertical thermal penetration and shallow enclosures may exhibit incomplete horizontal thermal penetration. According to the theoretical predictions<sup>14</sup>, the enclosure of the present experiment should feature distinct vertical thermal boundary layers, complete horizontal thermal penetration, and incomplete vertical thermal penetration. All these predictions were clearly justified by our experiments. In particular, the fact that, even though the aspect ratio of the apparatus is 0 (1), the fluid situated near, say, the top wall is practically at the same temperature as the warm region of the driving wall, unaffected by the presence of the cold region (incomplete vertical thermal penetration), stands out as an important result in itself. On the other hand, numerical simulations<sup>14</sup> for  $Pr=0.7$ ,  $H/L=1$ ,  $Ra=10^5$  did not show the existence of two flat cells along the two horizontal walls. Hence, it appears that these two cells constitute a feature of the high Rayleigh number regime.

### Acknowledgement

Financial support for this research provided by the University of Illinois Research Board and by NSF Grant no. ENG. 8451144 is greatly appreciated.

### References

1. **Catton I.** Natural convection in enclosures. *Seventh International Heat Transfer Conference, Toronto, 1978*, 6, 1979, 13-49
2. **Ostrach S.** Natural convection heat transfer in cavities and cells. *Keynote paper at the Seventh International Heat Transfer Conference, Munich, 1982*

3. **Ostrach S.** Natural convection in enclosures in *Advances in Heat Transfer*, 1972, **8**, 161–227
4. **Bejan A.** *Convection Heat Transfer*, John Wiley and Sons, New York, 1984, 159–201
5. **Chao P. K. B., Ozoe H., Churchill S. W. and Lior N.** Laminar natural convection in an inclined rectangular box with the lower surface half-insulated. *J. Heat Transfer*, 1983, **105**, 422–432
6. **Baker D. I.** A technique for the precise measurement of small velocities. *J. Fluid Mech.*, 1966, **26**, 573–575
7. **Kimura S. and Bejan A.** Experimental study of natural convection in a horizontal cylinder with different end temperatures. *Int. J. Heat Mass Transfer*, 1980, **23**, 1117–1126
8. **Sparrow E. M., Husar R. B. and Goldstein R. J.** Observation and other characteristics of thermals. *J. Fluid Mech.*, 1970, **41**, 793–800
9. **Eichhorn R., Leinhard J. H. and Chen C. C.** Natural convection from isothermal spheres immersed in a stratified fluid. *Proc. Fifth International Heat Transfer Conference, Tokyo, 1974, Paper NC1.3*
10. **Poulikakos D. and Bejan A.** Natural convection experiments in a triangular space. *J. Heat Transfer*, 1983, **105**, 652–655
11. **Kimura S.** Natural circulation in a horizontal duct with different end temperatures. *MS Thesis, University of Colorado at Boulder, May 1980*
12. **Imberger J., Thomson R. and Fandry C.** Selective withdrawal from a finite rectangular tank. *J. Fluid Mech.*, 1976, **78**, 489–512
13. **Lin N. N. and Bejan A.** Natural convection in a partially divided enclosure. *Int. J. Heat Mass Transfer*, 1983, **26**, 1867–1878
14. **Poulikakos D.** Natural convection in a confined fluid-filled space driven by a single vertical wall with warm and cold regions. *J. Heat Transfer*, 1985, **107**, 867–876